



## **Cyclic behaviour of full scale reinforced concrete bridge columns**

Luis F. Zuluaga Rubio<sup>1</sup>, Yoann Le Tartesse<sup>2</sup>, Christopher Calixte<sup>3</sup>, Georges Chancy<sup>4</sup>  
Patrick Paultre<sup>5</sup> and Jean Proulx<sup>5</sup>

<sup>1</sup> Junior Bridge Engineer, EXP, Montreal, QC, Canada.

<sup>2</sup> Field Engineer, H. Chevalier, Suresnes, France.

<sup>3</sup> Ph.D. Student, Department of Civil and Building Engineering, University of Sherbrooke, Sherbrooke, QC, Canada.

<sup>4</sup> Junior Engineer, WSP, Abitibi-Témiscamingue, QC, Canada.

<sup>5</sup> Professor, Department of Civil and Building Engineering, University of Sherbrooke, Sherbrooke, QC, Canada.

### **ABSTRACT**

Design procedures and guidelines for bridges under seismic loads have started to shift towards being performance-based to improve design and seismic risk assessment, with a strong scientific basis to make informed decisions. To implement this type of design, an accurate estimate of the damage limit states in terms of engineering criteria and experimental test results is especially important. Such an estimate requires, in turn, the consideration of the latest regulatory requirements in terms of confinement and transverse reinforcement, among others. Moreover, large-scale bridge component tests are essential to verify the reinforced concrete models developed based on small-scale specimen test results. This study presents a comparison between the experimental results of 4 real-scale reinforced concrete bridge columns, with different transverse reinforcement configurations, tested under constant axial load and reversed cyclic lateral loads. The column cross-sections correspond to the dimensions of a case study bridge located in Quebec, and the axial load used during the test was representative of the actual dead load of the bridge deck. In addition, a seismic assessment is presented by comparing the test results of each column with the limit states and the associated deformation levels for reinforced concrete bridge columns, prescribed in the Canadian Highway Bridge Design Code, CAN/CSA S6-14.

Keywords: cyclic behaviour, bridge column, confinement, ductility, limit states.

### **INTRODUCTION**

Bridges are the most critical components of the road transportation network. The functionality of bridges is given the highest priority for post seismic recovery actions. However, the documented damage caused by seismic events has underlined the necessity for an emergency plan for the road transport network, in which bridges play a fundamental role as the most vulnerable components of this network [1-2]. In the same manner, it is largely accepted that, in regular bridges, the columns are the main energy dissipating elements to withstand seismic effects [2]; thus, the study and understanding of the behaviour of these components under dynamic loads is fundamental for an adequate seismic assessment.

There has been a significant improvement in bridge design, mostly in earthquake bridge analysis and design, in the past few years [3-4]. The seismic analysis tools have improved, the seismic hazard maps have changed, and new codes and design procedures have been developed. The Canadian Highway Bridge Design Code [5] introduced insights on performance-based design philosophy in its 2006 version for the first time, and in the 2014 version, it became fully integrated. On the other hand, retrofit measures and mitigation strategies must be redefined for those existing bridges designed with codes and guidelines without the information now available on seismic safety. Furthermore, the availability of post seismic documented results as well as theoretical and experimental studies allow the implementation of the latter in new design codes for bridges and their components [4,6]. As a result, the traditional seismic design philosophy has started to shift towards the concept of performance-based earthquake engineering (PBEE) design, which seeks to improve seismic risk decision-making through assessment and design methods that have a strong scientific basis. A key feature in this process is the proper definition of performance limit states of the main components of the structure, such as bridge columns, that are relevant for seismic risk mitigation [2]. Consequently, due to the lack of systematic exploration for the accurate definition of bridge column limit states, an experimental research program was developed at the University of Sherbrooke to estimate the performance limit states of reinforced concrete bridge columns with different reinforcement details. As an essential part of this program, this study presents the experimental results of four real-scale reinforced concrete bridge columns subjected to lateral reversed



(a)



(b)

Figure 1: Chemin des Dalles Bridge: (a) overview; and (b) one bent view, [7].

cyclic loads and a constant axial load representing the real dead load. The column reproduces the exact geometric properties of the *Chemin des Dalles* bridge columns (Trois-Rivières, Quebec), as shown in Figure 1.

This paper also presents an assessment of the PBEE regulations by comparing the test results of each column with the limit states and the associated deformation levels for reinforced concrete bridge columns prescribed in the Canadian Highway Bridge Design Code [5].

## EXPERIMENTAL INVESTIGATION

### Test specimens

Four real-scale circular reinforced concrete columns were tested under combined constant axial load and reversed cyclic flexure. The column diameter was 914 mm, and the total height was 4600 mm, including a square rigid base foundation. The 1200 mm base foundation height was sufficient to anchor fifteen 35 mm diameter longitudinal bars. The column head was built with a square section, 600 mm high, to facilitate installation of horizontal hydraulic jacks. Lateral force was applied at a distance of 3100 mm from the top of the foundation. The specimens represent a 6.2 m high column in a typical bridge assuming that the point of contraflexure is located approximately at mid-column height. The concrete columns and foundation were cast vertically in two steps. The proper placement of the concrete was ensured with the use of a concrete vibrator. Figure 2 shows the experimental setup.



Figure 2: Experimental setup: as-built setup and specimen.

The nomenclature of the test specimens was defined as follows: the first letter is C for all columns, the second letter indicates the type of transverse reinforcement: H for hoops or S for spirals, followed by the transverse reinforcement spacing in millimeters (300 or 110 mm). The difference between specimens CH300 and CH300s is that the former is a replica of the real bridge column as built, i.e., with a lap splice at the base, whereas the latter did not have lapped splice at the base. Figure 3 shows the geometry and reinforcement of the four specimens.

### Test variables

The test variables were the lap splice at the base of the column (real bridge), no lap splice at the base of the column and circular hoops and spiral reinforcement spaced according to the new requirements of the Canadian bridge code [5]. Table 1 summarizes the specimen properties.

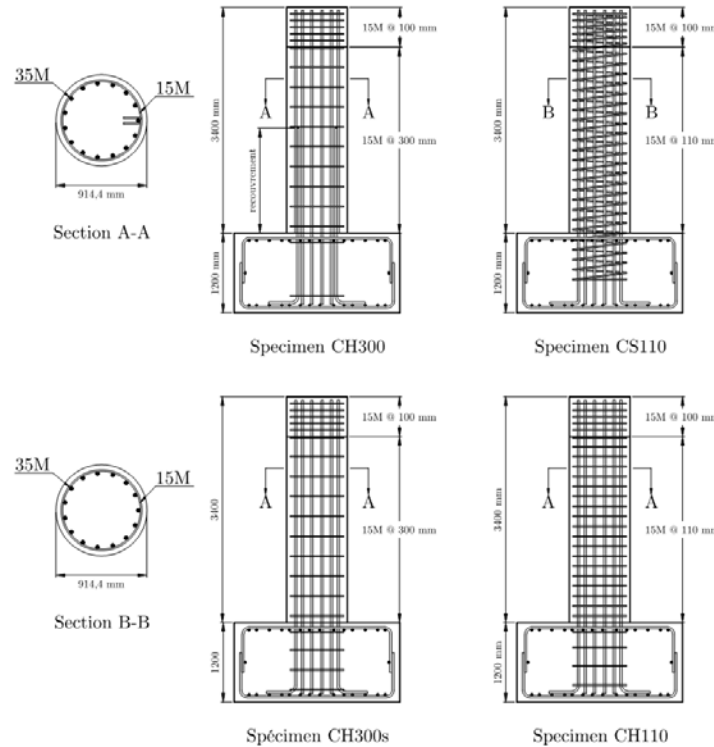


Figure 3: Specimen geometries.

Table 1. Specimen properties

Specimen	Reinforcement			
	Longitudinal	Transverse		
		Bars	Bars	Spacing (mm)
CH300†	35 M	15 M	300	Hoop
CS110	35 M	15 M	110	Spiral
CH110	35 M	15 M	110	Hoop
CH300s	35 M	15 M	300	Hoop

† Real bridge column replica.

### Reinforcing cages

Figure 3 provides details of the reinforcing cages. The longitudinal reinforcement includes 15-35 M Grade 400 weldable bars, which represents an average volumetric longitudinal reinforcement ratio of 2.00%. For both types of transverse reinforcement, hoops and spirals, 15 M Grade 400 weldable bars were used. The square column tip, where the lateral load was applied, was reinforced with square ties to prevent concrete crushing. The square foundation was designed to avoid excessive cracking and to provide proper anchorage for the longitudinal bars of the column.

### Instrumentation

To measure the global and local responses of the system, each specimen and their column-foundation joint were heavily instrumented. For the system global response, horizontal displacements at different column heights were measured from a fixed reference axis (an aluminum tower attached to the foundation). Additionally, the column rotation with respect to the top of the foundation was measured at different levels to obtain the column curvature distribution. Likewise, local deformations were measured along the predicted plastic hinges of the column and inside the column-foundation joint (longitudinal reinforcement strains at different levels and transverse reinforcement strains). All measurements were carried out using linear

variable displacement transducers (LVDTs) as well as potentiometers and electrical strain gauges installed on the steel rebars (longitudinal and transverse). The instrumentation was further improved and adjusted not only by considering the test evolution but also by anticipating the behaviour of the specimen according to the studied variables. All measurement devices were connected to a data acquisition system, which was also connected to the testing software used to control the hydraulic actuators. Figures 4 and 5 show the external and internal instrumentation, respectively, for all four specimens. Further information can be found in [8-11].

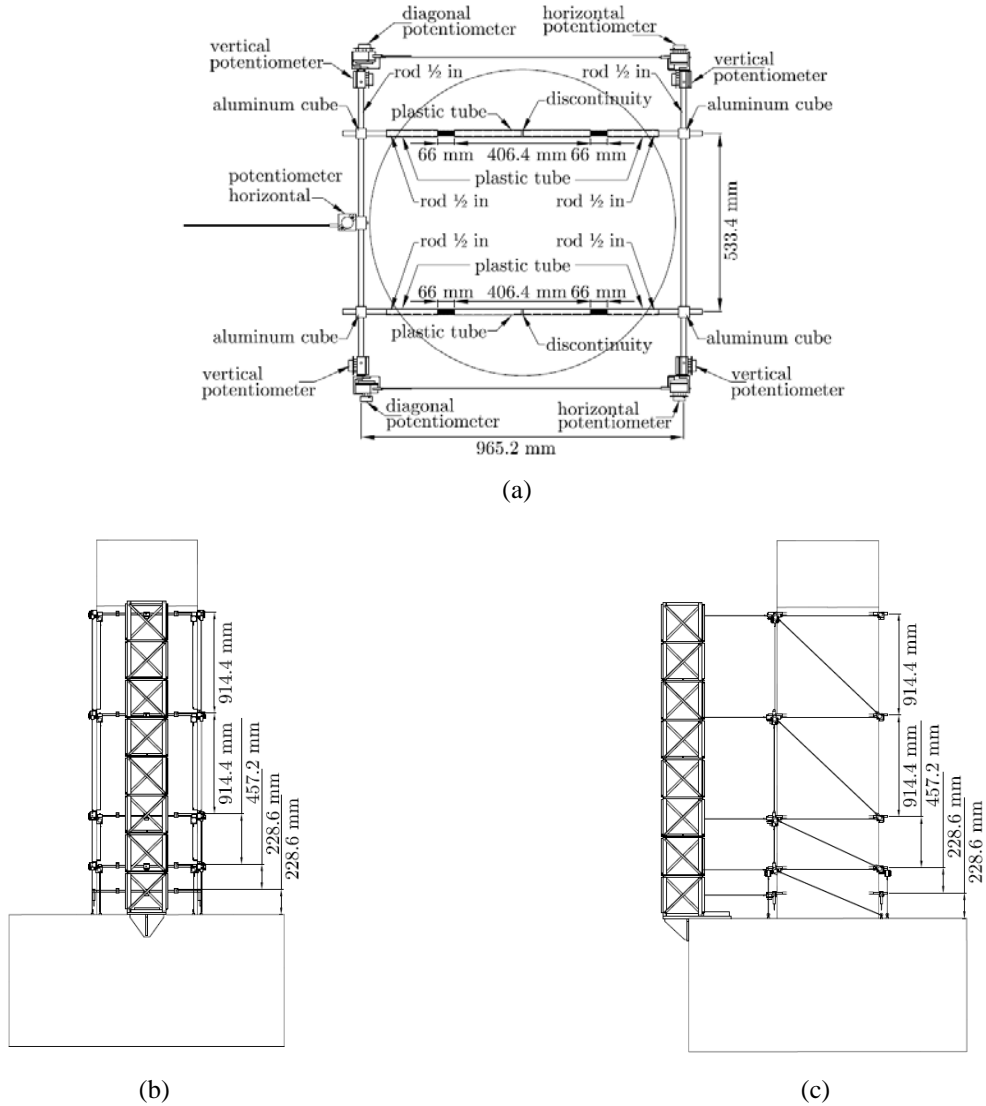


Figure 4: External instrumentation: (a) typical section plan view, (b) front elevation view, and (c) lateral elevation view

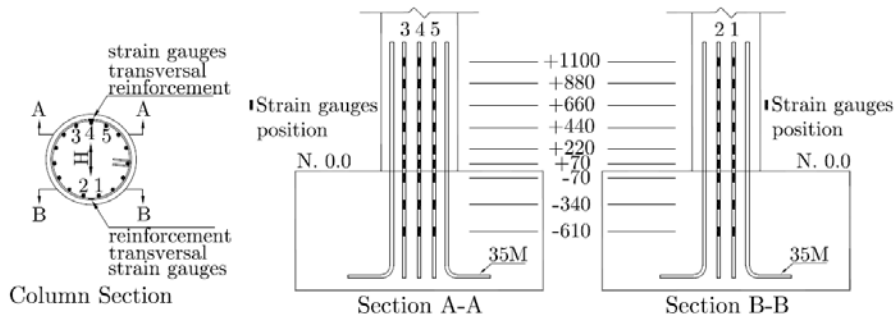


Figure 5: Internal instrumentation.

## Testing procedure

The axial load was applied until the target value of 2300 kN, which corresponds to the actual load acting on the bridge column prototype, was reached. The axial load remained constant during the test by controlling the force applied by two hydraulic actuators. After setting the axial load, the lateral cyclic loading started under displacement control. The first cycle was performed to attain 75% of the predicted yield displacement. The objective of this cycle was to crack the section. After completing this cycle, a second cycle was initiated to reach the yield displacement, defined as the point where the longitudinal bars first yielded in tension. Once the yield displacement was reached at each of the opposite sides of the column, the average of these values was defined as the experimental yield displacement. Next, the second cycle was repeated to reach the experimental yield displacement. Thereafter, for each successive load cycle, the experimental yield displacement was increased incrementally, as shown in Figure 6, and each displacement was repeated twice until column failure was reached. The test ended when at least one of the following events occurred: 1) the column was unable to sustain the axial load, characterized by a 10% loss of the applied axial load; 2) a drop of more than 50% of the maximum flexural capacity was observed; or 3) the longitudinal bar ruptured (due to buckling or tensile stress) or the transverse reinforcement ruptured, resulting in a significant drop in the flexural capacity.

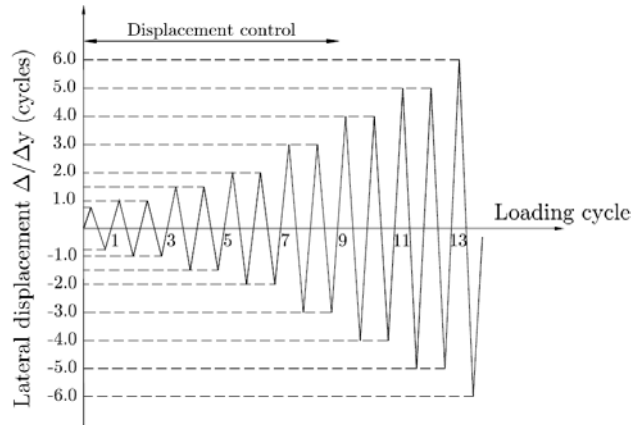


Figure 6: Loading protocol

## TEST RESULTS

### General behaviour

The specimen CH300 presented a 50% drop of the maximum flexural capacity as the test stop criterion. The other three specimens presented longitudinal bar buckling before the loss of capacity. As expected, the first cracks of all four specimens started in the first cycle, and as the lateral displacement demand increased, the distance between lateral cracks decreased. Additionally, for specimen CH300, vertical cracks appeared at the base of the column over the length of the lap spliced bars. Figure 7 shows the damage regions for all specimens at the end of the tests.

The yield strain was measured by the strain gauges installed on the longitudinal reinforcement before the concrete casting. The yield displacements (i.e., tip displacements corresponding to the measured yield strains),  $\Delta_{yexp}$ , are summarized in Table 2. The asymmetry of the longitudinal reinforcement explains the difference in the tip yield displacement between the load directions.

Table 2. Tip yield displacements

Lateral load direction	$\Delta_{yexp}$ (mm)			
	CH300	CS110	CH110	CH300s
South	14.46	18.67	15.94	20.10
North	18.01	19.33	17.14	19.60

Concrete crushing was observed in both the opposing lateral compression zones of the column, i.e., at the column-foundation interface. As the displacement demand increased, so did the height and thickness of the crushing zone towards the column core. Geometrically, the crushing zones described approximate arcs. One transverse and two longitudinal reinforcements were fully exposed at the column base in different cycles for three of the specimens,  $5\Delta_y$  for CH300,  $4\Delta_y$  for CS110 and  $6\Delta_y$

for CH110, where  $\Delta_y$  is defined as the yield displacement. The longitudinal reinforcement buckling took place for a tip displacement of 152 mm for CS110, 148 mm for CH110 and 120 mm for CH300s. As explained previously, CH300 did not show longitudinal reinforcement buckling (50% drop of the maximum flexural capacity was the test stop criterion).

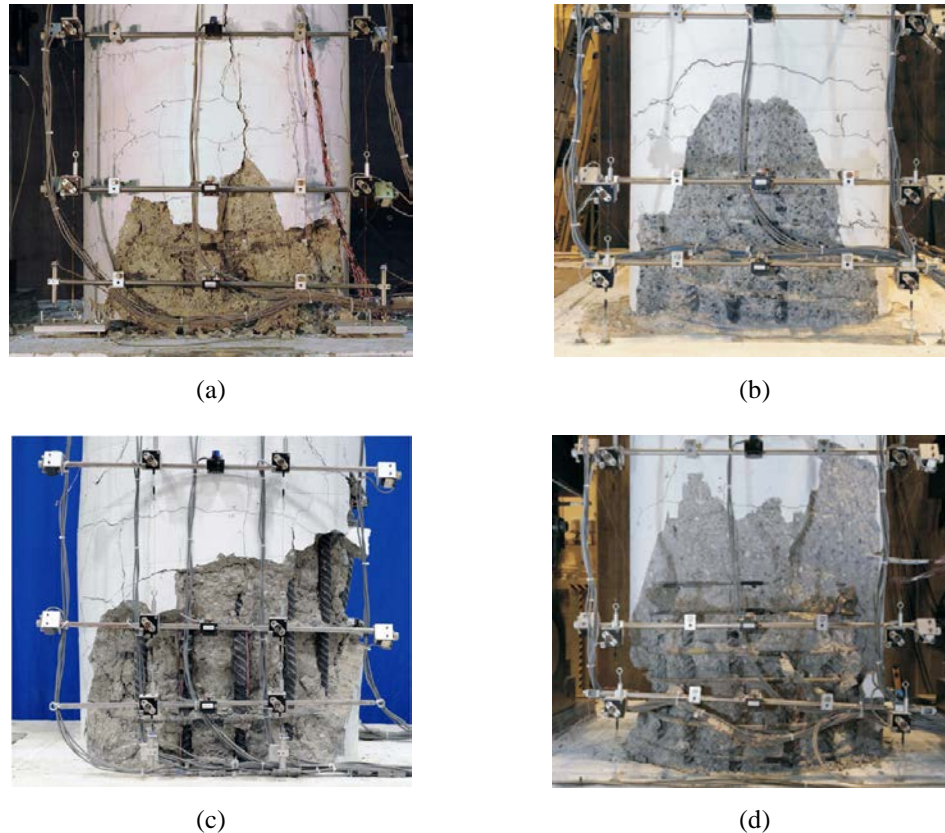


Figure 7: Damaged regions for all specimens: (a) CH300, (b) CS110, (c) CH300s, and (d) CH110.

Figure 8 shows the experimental force vs. tip displacement plot, whose enclosed area is related to the energy dissipation capacity. The specimens showing more dissipation and displacement capacity are those with closer transversal reinforcement spacing, following the actual provisions of the Canadian Highway Bridge Design Code [5]. However, for all specimens, the maximum lateral force sustained is approximately equal. Additionally, from the test results of specimens CS110 and CH110, the difference between a continuous transverse reinforcement (spiral) and individual circular hoops is not significant, as long as small transverse spacing is provided. The pinching effect observed in specimen CH300 is caused by the lap splice at the column base when combined with a large transverse spacing.

### Limit states and performance levels

Identification of the limit states that are relevant to the system performance is fundamental for the implementation of the PBEE design [12]. In the presence of a strong seismic event, reinforced concrete bridges may be damaged in different ways, among them, the most typical are (i) cracking, (ii) yielding of longitudinal reinforcements, (iii) spalling of concrete cover or concrete crushing, (iv) rupture of transverse reinforcements, (v) buckling and rupture of longitudinal reinforcements, and (vi) confined core degradation. Taking into account the experimental test results, the present study was focused on quantifying the column performance levels associated with damage states (i) to (v) mentioned above. Based on the qualitative descriptions of the expected performance associated with the structural damage, reinforced concrete bridge performance levels are defined as follows: immediate or fully operational, limited or operational, service disruption, life safety or near collapse and collapse.

Hose and Seible [13] determined the bridge performance parameters associated to the design parameter levels. Their results are shown in Table 3. Following the same approach as Hose and Seible [13], and based on the results of this research, Table 4 presents the average performance parameter values for the four specimens according to the measured parameter levels. The main parameters used to relate to the performance levels are steel strain, concrete strain, drift and displacement ductility. Usually, the drift is considered to be a good parameter to express the performance levels.

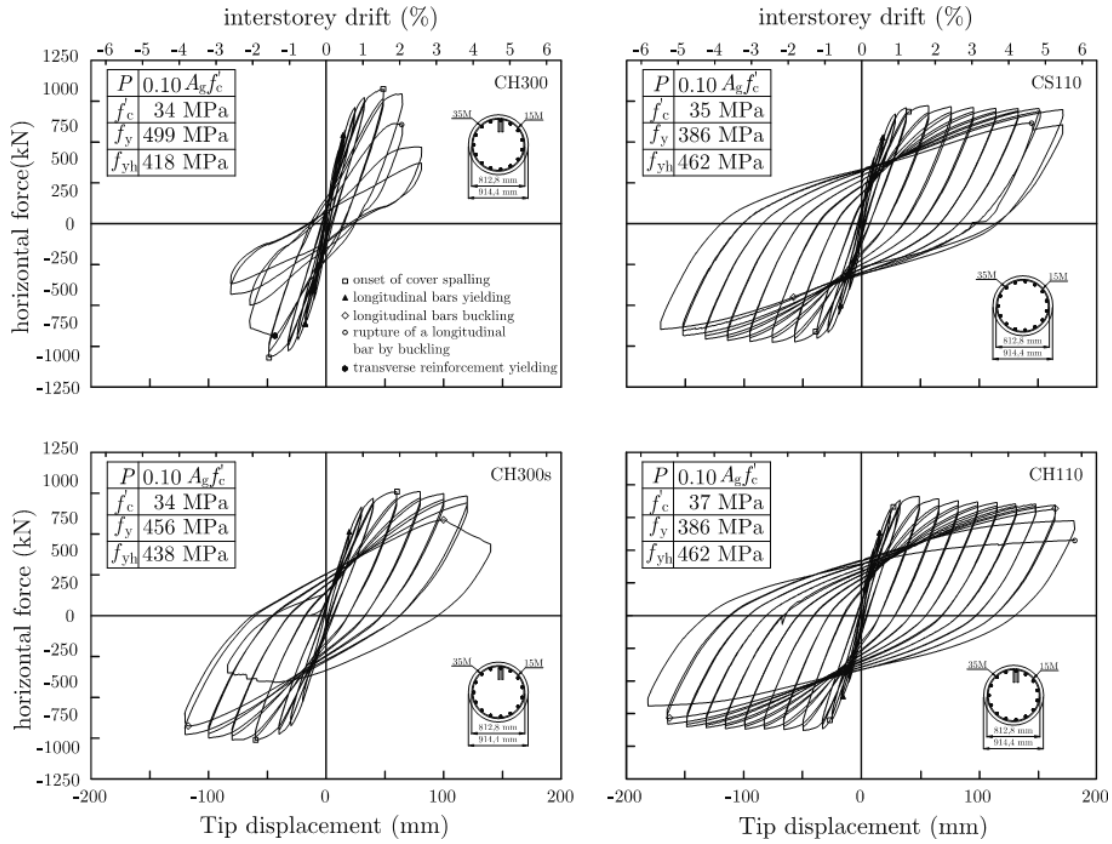


Figure 8: Experimental and monotonic predictions of moment-curvature responses

Table 3. Bridge performance/design parameters (Hose and Seible [13])

Level	Description	Steel strain	Concrete strain	$\Delta/L$ (%)
I	Fully operational	<0.005	<0.0032	<1.0
II	Operational	0.005	0.0032	1.0
III	Life safety	0.019	0.0100	3.0
IV	Near collapse	0.0480	0.0270	6.0
V	Collapse	0.0630	0.0360	8.0

Table 4 presents the performance parameters in terms steel strain, concrete strain and drift for the tested four specimens. When comparing Tables 3 and 4, it can be seen that the results are close. The main difference could be explained by the fact that specimen CH300 has a known fragile lap splice detail at the base, but was included in the calculation of the average values. Furthermore, the collapse level depended on criteria that was defined before performing the tests.

Table 4. Bridge performance/measured parameters for the tested four specimens

Level	Description	Steel strain	Concrete strain	$\Delta/L$ (%)
I	Fully operational	<0.0037	<0.0023	<1.0
II	Operational	0.0037	0.0023	1.0
III	Life safety	0.0060	0.0035	1.9
IV	Near collapse	0.0302	N.M.	4.0
V	Collapse	N.M.	N.M.	4.8

## CONCLUSIONS

The main objective of this study was to address the significant uncertainties that remain in the quantitative definition of the reinforced concrete bridge column limit states, particularly at the associated deformation levels. Accordingly, this paper presents the experimental results of four real-scale reinforced concrete bridge columns, with different transverse reinforcement configurations, submitted to lateral cyclic loads in addition to a constant axial load representing the real dead load. In addition to the comparison of the general behaviour between the specimens, the experimental lateral force-tip displacement curves were also displayed, showing the effect of transverse reinforcement in the concrete confinement and in the cyclic behaviour. The damaged regions at the end of the tests showed that the damage states of the four specimens are similar and occur in the same order: cracking, yielding of longitudinal bars, beginning of concrete crushing, concrete cover loss and yielding of transverse reinforcement. The test results also showed the detrimental of using lap splice at the base of a bridge pier. This paper also included a comparison of the experimental limit states of each column with the limit states and the associated deformation levels for reinforced concrete bridge columns prescribed in the regulatory guidelines. Within this PBEE framework, it is believed that the results presented herein will be useful for improving the seismic evaluation of existing bridges in Canada's road networks and for optimizing the seismic design of future structures according to the performance-based seismic approach.

## ACKNOWLEDGMENTS

The authors would like to acknowledge the financial support of the Ministry of Transportation of Quebec (MTQ), the Natural Sciences and Engineering Research Council of Canada (NSERC), the Quebec Fonds pour la Recherche sur la Nature et les Technologies (FQRNT), the Centre d'études interuniversitaire des structures sous charges extrêmes (CEISCE) and the Centre de recherche en génie parasismique et en dynamique des structures (CRGP) of the Université de Sherbrooke. The authors would also like to acknowledge the collaboration of Laurent Thibodeau, Jason Desmarais, Claude Aubé, Raphaël Prévost, Éric Beaudoin and Antony Bergeron, technicians in the Department of Civil Engineering at Sherbrooke University, for their role in the test preparation and during the tests.

## REFERENCES

- [1] Paultre, P., Tavares, D., Suescun, J. and Padgett, J.E. (2013). "Seismic fragility of a highway bridge in Quebec". *Journal of bridge engineering*, **18**(11):1131-1139.
- [2] Tavares, D., Padgett, J.E. and Paultre, P. (2012). "Fragility curves of typical as-built highway bridges in eastern Canada". *Engineering Structures*, **40**(7):107-118.
- [3] Siqueira, G., Sanda, A., Paultre, P. and Padgett, J.E. (2014). "Fragility curves for isolated bridges in eastern Canada using experimental results". *Engineering Structures*, **74**(9):311 - 324.
- [4] Siqueira, G., Tavares, D., Paultre, P. and Padgett, J.E. (2014). "Performance evaluation of natural rubber seismic isolators as a retrofit measure for typical multi-span concrete bridges in eastern Canada". *Engineering Structures*, **74**(9):300 - 310.
- [5] Canadian Standard Association (2014). "Canadian Highway Bridge Design Code. CAN/CSA-S6-14". Mississauga, ON, Canada.
- [6] Priestley, M. J. N., Seible, F. and Calvi, G. M. (1996). "Seismic design and retrofit of bridges". Wiley, New York.
- [7] Roy, N. (2006). "Réhabilitation parasismique performantielle des ponts avec des polymères renforcés de fibres de carbone". Ph.D. Thesis, Université de Sherbrooke, Sherbrooke, QC, CANADA.
- [8] Calixte, C. (2015). "États limites de piliers de ponts en béton armés d'armatures en spires hélicoïdales". Master's thesis, Université de Sherbrooke.
- [9] Chancy, G. (2015). "États limites de piliers de ponts en béton armés de cerces". Master's thesis, Université de Sherbrooke.
- [10] Le Tartesse, Y. (2018). "Étude de l'influence du chevauchement des barres d'armatures d'un pilier de pont en béton armé". Master's thesis, Université de Sherbrooke.
- [11] Zuluaga, L. (2015). "États limites de piliers de ponts en béton armés de cerces avec recouvrement à la base". Master's thesis, Université de Sherbrooke, 2015.
- [12] Lehman, D., Moehle, J., Mahin, S., Calderone, A., and Henry, L. (2004). "Experimental evaluation of the seismic performance of reinforced concrete bridge columns". *Journal of Structural Engineering*, **130**(6), 869–879.
- [13] Hose, Y.D. and F. Seible, F. (1999). "Performance Evaluation Database for Concrete Bridge Components and Systems under Simulated Seismic Loads". Pacific Earthquake Engineering Research Center, Berkeley, California.